RSC Advances

This is an *Accepted Manuscript*, which has been through the Royal Society of Chemistry peer review process and has been accepted for publication.

Accepted Manuscripts are published online shortly after acceptance, before technical editing, formatting and proof reading. Using this free service, authors can make their results available to the community, in citable form, before we publish the edited article. This *Accepted Manuscript* will be replaced by the edited, formatted and paginated article as soon as this is available.

You can find more information about *Accepted Manuscripts* in the Information for Authors.

Please note that technical editing may introduce minor changes to the text and/or graphics, which may alter content. The journal's standard Terms & Conditions and the Ethical guidelines still apply. In no event shall the Royal Society of Chemistry be held responsible for any errors or omissions in this *Accepted Manuscript* or any consequences arising from the use of any information it contains.

ROYAL SOCIETY OF CHEMISTRY

www.rsc.org/advances

Charge Transfer and Dipole Formation at Silver Nanoparticle-Tetracyanoquinoid takes place in the solid-state membrane, forming an unprecedented, highly olefin permselective facilitated transport membrane with a mixed gas selectivity over 100 for a propylene/propane mixture. This provides a potential alternative to the highly energy-intensive cryogenic distillation process for olefin/paraffin separation.

Keyword: silver metal, TCNQ, F4-TCNQ, olefin, facilitated transport

Il Seok Chae, Sang Wook Kang* and Yong Soo Kang*

Olefin Separation via Charge Transfer and Dipole Formation at Silver Nanoparticle-Tetracyanoquinoid Interface

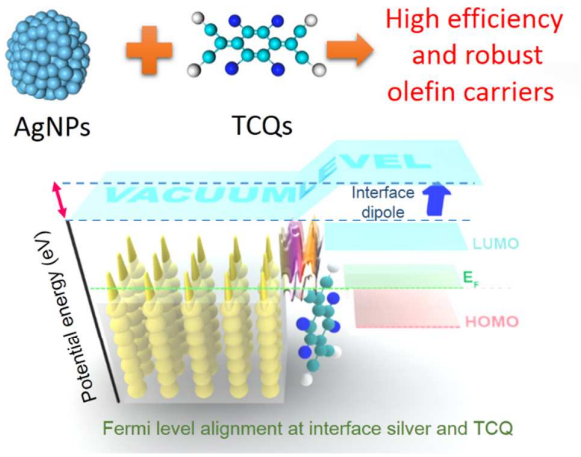

RSC Advances Accepted Manuscript

Journal Name

RSCPublishing

ARTICLE

Olefin Separation via Charge Transfer and Dipole Formation at the Silver Nanoparticle-Tetracyanoquinoid Interface

Cite this: DOI: 10.1039/xoxxoooooox

Il Seok Chae, [a] Sang Wook Kang,*[b] and Yong Soo Kang*[a]

Received ooth January 2012,
Accepted ooth January 2012

DOI: 10.1039/xoxxoooooox

www.rsc.org/

In this study, we report the significantly increased carrier activity of AgNPs in silver-olefin complexation, induced by the addition of tetracyanoquinoidal molecules (TCQs) such as TCNQ and F4-TCNQ. The interaction between AgNPs and TCQs were investigated by UV-Vis spectroscopy. The Kelvin probe and XPS data revealed vacuum level shifts and dipole formation at the AgNPs/TCQs interface, resulting in the increased work function of the AgNPs from 4.89 up to 5.25 eV. As a result, membranes containing AgNPs/TCQs demonstrated a mixed gas selectivity of *ca*. 100 for a 50/50 (vol%) propylene/propane mixture and showed stable performances.

Introduction

The advent of membrane technology is bringing us closer to solving the environmental and energy-related issues, in dealing with CO_2 capture, natural gas purification and water purification.[1] Recently, Koros *et al.* reported that the membrane filtration technology is 10 times energetically more efficient than the conventional thermal desalination method for water purification.[2] Similarly, membrane-based gas separation systems also offer certain unique features, such as simple operation, space-saving, and no phase transition of chemical components. Such membrane-based gas separation systems are expected to dramatically reduce the energy consumption, compared with the conventional gas separation operations such as cryogenic distillation and adsorption processes.[3] During the various gas separation processes, light olefins such as ethylene and propylene are typically produced *via* highly energy-intensive cryogenic distillation. They are the most important and largest feedstock in the petrochemical industry.[4] Herein, we report the formation of an unprecedented olefin permselective membrane, utilizing the charge transport and dipole formation at the organic/silver interface.

Thus far, several kinds of membranes have been studied for the separation of olefin/paraffin.[5] However, the close physicochemical properties of olefin and paraffin, such as their molecular size and solubility, generally have limited membrane processes governed by solution–diffusion mechanisms. Lately, facilitated olefin transport membranes have received much attention because of their unique mass transport phenomena.[6] This facilitated transport is particularly feasible when a chemical compound in the membrane interacts reversibly with a specific solute. It acts as the so-called carrier for the solute, resulting in the carrier-mediated transport. In addition to the carrier-mediated transport, Fickian transport also occurs by means of concentration gradient. Accordingly, the total transport of the solute will be facilitated by the synergistic effect of carrier-mediated and Fickian transport, proving it to be a very attractive strategy for improving the separation performances of olefin/paraffin mixtures.

More recently, research on charge transport and dipole formation at the organic/metal interface has gained significant importance in designing new functional materials for novel applications,[7] including the facilitated transport membranes.[8] In case of olefin/paraffin separation, the typical olefin carriers are silver cations (Ag^+). However, silver ions are readily reduced to silver nanoparticles, which result in the poisoned carrier activity.[9] Given these considerations, our group recently demonstrated that the silver metal nanoparticles (AgNPs) could be made to interact with olefins such as propylene and ethylene, and act as olefin carriers for facilitated transport, if they are activated to carry a positive surface charge. This is based on the fact that the Ag^+ ions exhibit strong reversible interactions with olefin molecules. For example, poly(ethylene-*co*-propylene)/AgNPs/*p*-benzoquinone membrane is reported to demonstrate a propylene/propane selectivity of 11 and a total mixed gas permeance of 0.5 GPU (1 GPU = 1×10^{-6} cm^3 (STP)/(cm^2 s cmHg)). Here, the electron acceptor *p*-benzoquinone caused the partial positive polarization of the surface of the AgNPs.[8a] Furthermore, recent studies have reported that the gas separation performance of a membrane-based system depends on the nature of the electron acceptor used in the membrane, which determines the partial positive

RSC Advances Accepted Manuscript

charge on the surface of silver nanoparticle. It has been demonstrated that the presence of strong organic electron acceptor, such as 7,7,8,8-tetracyanoquinodimethane (TCNQ), induces high positive charge density on the surface of AgNPs, resulting in propylene/propane selectivity of up to 50. In that study, the concentration of AgNPs was maintained as 50 wt.% with respect to the polymer matrix.[8b]

In the present study, we report the preparation of significantly enhanced olefin separation membrane, by taking advantage of the excellent charge transport properties of tetracyanoquinoidal molecules (TCQs) and utilizing the high AgNPs concentration of up to 100 wt.% of the polymer matrix. The resulting membrane demonstrated a propylene/propane separation factor of over 100. Moreover, we have also explored the charge transfer and dipole formation phenomena at interface of AgNPs with varying concentration of TCQs, in terms of the electronic structure. Systematic investigations performed by using UV-Vis spectroscopy, Kelvin Probe, XPS, and TEM, have indicated the optimized conditions, such as the weight ratio and the type of electron acceptor, thus allowing the establishment of a novel, high efficiency, and simple fabrication of nanocomposite membrane for facilitated olefin transport.

Experimental

Materials

Silver tetrafluoroborate ($AgBF_4$, 98%) was used as the precursor for the synthesis of Ag particles, while poly(vinylpyrrolidone) (PVP, K28~32) was used as the stabilizer and the membrane matrix. Ethanol (EtOH) was used as a solvent, while 7,7,8,8-tetracyanoquinodimethane (TCNQ) and 2,3,5,6-tetrafluoro-7,7,8,8-tetracyanoquinodimethane (F4-TCNQ) were used electron acceptors to induce positive charge on the surface of the silver particles. All of the chemicals were used as received from Aldrich Chemical Co.

Preparation of PVP/AgNPs/TCQs nanocomposite

In this study, the AgNPs were prepared by a simple reflux method. Subsequently, PVP/AgNPs/TCQs nanocomposite was synthesized, as described by the following procedure. Silver tetrafluoroborate solution A was prepared by adding 1.7g of $AgBF_4$ to 30 ml EtOH. Solution B was prepared by dissolving 1g of PVP in 30 ml EtOH, which was subsequently heated to 80°C under vigorous stirring. Following that the solution A was added dropwise into solution B under refluxing condition. The resulting mixture (AgNPs) was stirred continuously at 70°C for 6 h. Following that, 0.1, 0.05, and 0.02 g of TCQs were added to the mixed solution. After incorporating TCQs, the mixed solution was stirred sufficiently to form the surface dipole at the AgNPs/TCQs interface. Note that no special process was adopted to separate AgNPs. The EtOH was evaporated, and dried in vacuum. Finally, PVP/AgNPs/TCQs were obtained as dried film powder.

Nanocomposite PVP/AgNPs/TCQs membranes were prepared by dissolving 0.2g of the as-prepared PVP/AgNPs/TCQs in 0.8g of EtOH. The resulting solution were then coated onto commercial macroporous polysulfone membrane support (Woongjin Chemical Industries Inc., Seoul, Korea) using an RK Control Coater (Model 101, Control Coater RK Print-Coat Instruments Ltd., UK). The average pore size of the surface of the macroporous membrane support was 0.1 μm, while the thickness was approximately 40 μm for the asymmetric structure. The selective layer was estimated to be ca. 20 μm by the EDX attached to SEM. After the solvent was evaporated in a convection oven at room temperature (RT) under N_2, the PVP/AgNPs/TCQs composite membranes were dried completely in a vacuum oven for two days at RT.

Characterization

The morphology of the silver nanoparticles that were obtained by the reduction of silver ions was observed by using transmission electron microscope (TEM, JEOL JEM-3010), operating at 300 kV. Specimens for TEM were prepared by placing a drop of the ethanol solution containing PVP and Ag^o onto a standard TEM copper grid. The UV-vis absorption spectra were recorded using an Optzen 2120 UV spectrophotometer with a 5nm resolution. X-ray photoelectron spectroscopic (XPS) data were acquired using a Perkin-Elmer Physical Electronics PHI 5400 X-ray photoelectron spectrometer. This system was equipped with a Mg X-ray source operating at 300 W (15 kV, 20 mA). The carbon (C 1s) line at 285.0 eV was used as the reference for determining the binding energies. The work function data were acquired using the McAllister Technical Services KP-6500 Kelvin probe system.

Separation performance

The 50:50 propylene/propane mixed gas separation properties of the PVP/AgNPs/TCNQ and F4-TCNQ composite membranes with a membrane area of 2.25 cm^2 were evaluated by using a gas chromatograph (Hewlett–Packard G1530A, MA) equipped with a TCD detector and a unibead 2S 60/80 packed column. Gas flow rates and gas permeances were measured with a mass flow meter.

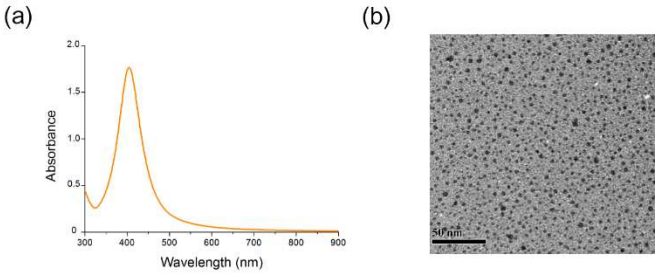

Figure 1. (a) UV-Vis absorption spectra of PVP-capped AgNPs in EtOH. (b) Transmission electron microscopic image of AgNPs.

Results and Discussion

Preparation of PVP-capped AgNPs

Silver nanoparticles were prepared at a fixed molar ratio of [C=O]:Ag^+= 1:1. In the typical process, a colorless solution of PVP in ethanol was mixed with $AgBF_4$, which immediately resulted in the formation of bright yellow colored AgNPs. As the lattice energy of $AgBF_4$ is low, the kinetic of AgNPs formation is considered to be fast. The formation of AgNPs was confirmed from the surface plasmon resonance (SPR) peak at about 400 nm, as can be seen from the UV-Vis spectrum of the sample shown in Fig. 1 (a). With subsequent heat treatment for 30 min, the SPR peak became sharp and narrow, indicating the formation of PVP-stabilized silver nanoparticles with a narrow size distribution. The TEM image of the as-prepared silver

RSC Advances Accepted Manuscript

 This journal is © The Royal Society of Chemistry 2012

nanoparticles is shown as Fig. 1 (b), revealing an average particle size of 5 nm with a standard deviation of 2 nm.

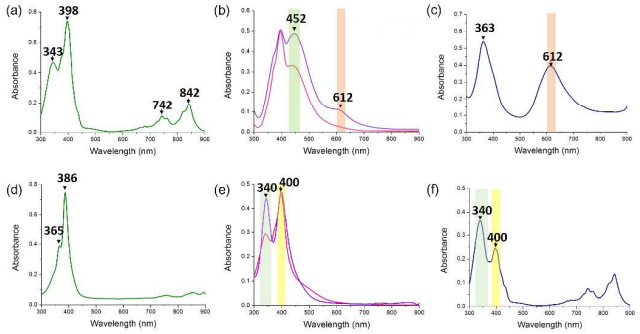

Figure 2. UV-Vis spectra of TCQs and the PVP/AgNPs/TCQs membrane in EtOH solution. (a) TCNQ (0.01 mM), (b) Pink: PVP/AgNPs/TCNQ = 1:1:0.02; Purple: PVP/AgNPs/TCNQ = 1:1:0.05, (c) PVP/AgNPs/TCNQ = 1:1:0.1, (d) F4-TCNQ (0.01 mM), (e) Pink: PVP/AgNPs/F4-TCNQ = 1:1:0.02; Purple: PVP/AgNPs/F4-TCNQ = 1:1:0.05, (f) PVP/AgNPs/TCNQ = 1:1:0.1.

Interaction between AgNPs and TCQs molecule.

The interactions between the AgNPs and TCQs molecules (TCNQ, F4-TCNQ) were investigated by using UV-Vis spectroscopy, as shown in Fig. 2. It is well known that the UV-Vis spectra of quinoidal compounds are dominated by the HOMO-LUMO electronic structure, and that the peaks of its radical anion form are strongly red-shifted in comparison with neutral molecules.[10] Therefore, the changes in the electronic structure of the molecules could be clearly observed through the UV-Vis analysis.

The UV-Vis spectra of TCNQ and F4-TCNQ are shown in Fig. 2 (a) and Fig. 2 (d), respectively. The UV-Vis spectra of TCNQ solution (Fig. 2 (a)) has 3 peaks, namely, one strong absorption at *ca.* 400 nm, and two less intense peaks in the spectral range of 300–370 nm and 600–900nm. Similarly, the UV-Vis spectra of F4-TCNQ (Fig. 2 (d)) also showed 3 peaks, with a strong absorption peak at around 386 nm. Although the molecular structure of F4-TCNQ is analogous to TCNQ, they have a minute difference in the electronic structure. Therefore, we analyzed the UV-Vis studies of TCNQ and F4-TCNQ reported in the literature and the results are summarized in the Table 1.

Furthermore, we investigated the changes in the UV spectra, caused as a result of interactions between the AgNPs and TCQs. Fig. 2 (b) shows the UV-Vis spectra of different concentrations of TCNQ in PVP/AgNPs solution. Upon mixing the PVP/AgNPs solution with TCNQ solution, the absorption peak corresponding to the TCNQ radical anion at around 800 nm disappeared immediately, followed by the appearance of a new band in the range of 420–460 nm. To gain further insight on this behavior, we introduced more than twice the amount of TCNQ into the sample. This resulted in an increase in the intensity of the peak at around 452 nm, which corresponds to $TCNQ^{\bullet-}$. In addition, we could observe the appearance of another peak at around 624 nm. Similar trend was observed in case of F4-TCNQ, as shown in Fig. 2 (e). In both the concentrations of F4-TCNQ, there occurred a new developing band at around 340 nm, which could be assigned to $F4\text{-}TCNQ^{2-}$. In both the TCQ samples, the peak at 400 nm was almost unchanged, suggesting that this peak could be mainly attributed to the AgNPs formed in the system.

Table 1. UV-Vis absorption of TCQs molecules and their reduced species.

	λ_{max} (nm)[1)]		λ_{max} (nm)[2)]
TCNQ	399[a]	F4-TCNQ	386
$TCNQ^{\bullet-}$	420[a],441[b],690[b],761[c],842[a]	F4-$TCNQ^{\bullet-}$	410, 754, 856
$TCNQ^{2-}$	334[c]	F4-$TCNQ^{2-}$	335

1) References a: [10a], b: [10b], c: [10c,d]

2) All the UV-Vis data of F4-TCNQ and its reduced species were obtained from ref [10b]

Upon introducing a considerable amount of TCQ (up to 10 wt % of AgNPs), a new peak was found in both TCNQ and F4-TCNQ. In case of TCNQ, the peak at around 452 nm was no longer observed in Fig. 2 (c). However, there were two peaks at around 370 and 624 nm in the spectral ranges of 300–440 nm and 540–760nm, respectively. This is in good agreement with those reported for AgTCNQ nanowire.[11] On the other hand, in case of F4-TCNQ, the peak at 340 nm corresponding to the $F4\text{-}TCNQ^{2-}$ was found to increase with the addition of TCQ. In addition, we could observe the development of $F4\text{-}TCNQ^{\bullet-}$ in the spectral range of 600–900 nm.

The above phenomena suggest that the electron transfer from AgNPs to TCQs varies depending on the nature of electron acceptor and weight ratio. One electron transfer occurs in case of TCNQ, whereas two electrons transfer between F4-TCNQ and AgNPs. Also, in the case of PVP/AgNPs/TCNQ= 1:1:0.1 (wt. ratio), the morphology change of Ag metal was expected. However, the absorption band at around 400 nm was still observed in PVP/AgNPs/F4-TCNQ=1:1:0.1 (wt. ratio), suggesting that the spherical shape of Ag metal is still maintained.

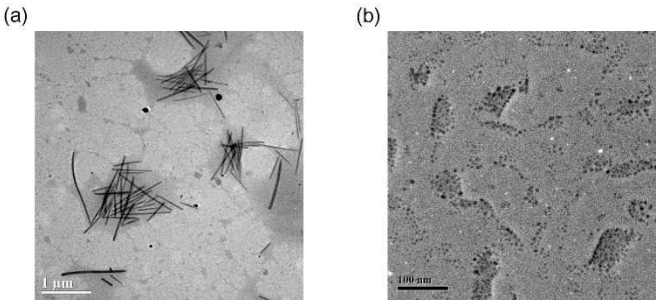

Figure 3. TEM images of the PVP/AgNPs/TCQs nanocomposite membranes: (a) PVP/AgNPs/TCNQ = 1:1:0.1 and (b) PVP/AgNPs/F4-TCNQ = 1:1:0.1.

Changes in the morphology of AgNPs upon addition of TCQ molecule.

The abovementioned results were further verified from the corresponding TEM images shown in Fig. 3. The TEM image of the PVP/AgNPs/TCQs shown in Fig. 3 (a) indicates that the diameter of the nanorod is ~ 20 nm, while the length is < 1 μm. The corresponding energy-dispersive X-ray spectroscopic

RSC Advances Accepted Manuscript

(EDS) analysis of the nanorod indicated the presence of C, N, and Ag. In addition, the nanowire contained the element O due to the presence of polymer PVP, although it was not observed as crystal state in the TEM image. Accordingly, the nanorods are believed to have formed by the so-called spontaneous process[11b], wherein neutral TCNQ molecules react with the PVP-capped AgNPs. On the other hand, assembled AgNPs were observed in case of PVP/AgNPs/F4-TCNQ = 1:1:0.1 (wt. ratio), however, no significant change was observed, as shown in Fig. 3 (b).

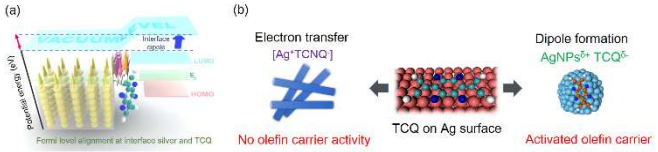

Scheme 1. Schematic illustration of (a) Principle underlying the work function change in terms of energy diagram at the organic/metal electron acceptor interface. After charge transfer, the complex between electron acceptor and silver, and their corresponding Fermi levels are in equilibrium. Consequently, the vacuum level is shifted by the interface dipole. (Modified from G. Heimel *et al.*[7] and previous report [8b]) (b) The proposed morphology change that occurs due to the strong interaction between Ag atoms and TCNQ, and the partial positive charge formation due to the interaction between AgNPs and TCQs molecules.

Change in the work function of AgNPs

The work functions of AgNPs without TCQs in PVP matrix were measured by using Kelvin probe system. The change in work function can be ascribed as follows: i) the formation of dipole layer due to the charge transfer complex at the metal/organic interface, and ii) vacuum level (VL) shift occurs as much as dipole layer by Fermi energy level alignment between metal and organic molecule.[7] (Scheme.1 (a)) In this manner, the outer atomic layer of a metal can be polarized to be positive or negative, analogous to the tunable work function of electrode in optoelectronic devices.

The introduction of TCNQ or F4-TCNQ into the PVP/AgNP composite membrane leads to changes in the work function of Ag. As shown in Table 2, the maximum increase in the work function of Ag was observed upon the addition of 0.05 wt. ratio of F4-TCNQ, while the minimum increase in work function was observed with the introduction of 0.02 wt. ratio of TCNQ. Such an increase in the work function can be attributed to the interfacial electronic structure and interface dipole at AgNPs/TCQs (Scheme.1). The larger increase in the work function in case of F4-TCNQ when compared with TCNQ can be attributed to the two electrons transfer or the dipole formation at $AgNPs^{\delta+}$/ $F4\text{-}TCNQ^{2-}$.

In case of PVP/Ag^{o}/TCNQ = 1:1:0.1 (wt. ratio), the work function of Ag decreased from 4.89 to 4.81. Presumably, the nanowire-shaped Ag^{o}/TCNQ might have a repeating period along the p–p stacking direction, which is generally observed in a highly anisotropic AgTCNQ crystal. Thus, it appears that the dipole formation is difficult in the stacked Ag–TCNQ molecules with large p–p overlap. [11c]

Table 2. Ag work functions [eV] of the PVP/AgNP membranes containing different TCQs compositions.

Membrane type	Ag work function (ϕ)	Δϕ [1)]
PVP/Ag		
1 : 1	4.89	
PVP/Ag/TCNQ		
1 : 1 : 0.02	5.14	+ 0.25
1 : 1 : 0.05	5.15	+ 0.26
1 : 1 : 0.10	4.82	– 0.07
PVP/Ag/F4-TCNQ		
1 : 1 : 0.02	5.21	+ 0.32
1 : 1 : 0.05	5.25	+ 0.36
1 : 1 : 0.10	5.24	+ 0.35

1) Work function difference relative to 'PVP/Ag' sample.

XPS analysis of AgNPs in PVP/AgNPs/TCQs

The changes in the chemical environment around AgNPs/TCQs were analyzed by using X-ray photoelectron spectroscopy (XPS). In addition, the formation of partial positive charges on the surface was also confirmed from the XPS analysis. Fig. 4 (a) shows the changes in the binding energy of the $d_{5/2}$ orbital of Ag, upon the introduction of TCNQ or F4-TCNQ in the PVP-Ag^{o} composite system. Note that the binding energy of metallic Ag and PVP-stabilized AgNPs were reported to be 368.26 and 368.31 eV, respectively.[8] Upon addition of 0.02 wt. ratio of TCQs to the PVP/AgNP composite membrane, the binding energy of PVP/Ag^{o}/TCNQ and PVP/Ag^{o}/F4-TCNQ composite system increased up to 369.01 eV and 369.05 eV, respectively. This indicates that the TCQs induce positive charge density on the nanoparticles, which in turn increases the valence electrons in the silver atoms. However, when 0.1 wt. ratio of TCNQ was added, the binding energy decreased to 368.65 eV. Presumably, this could be due to the Ag^{+} existing with $TCNQ^{-}$, and not the positive polarized AgNPs. On the other hand, the $d_{3/2}$ orbital of Ag increased in case of F4-TCNQ when compared with that of PVP/Ag^{o}/F4-TCNQ= 1:1:0.2, whereas almost similar value was observed in $d_{5/2}$ orbital of Ag. This could be explained considering the interactions between the silver atoms and TCQs, which is consistent with the work function data.

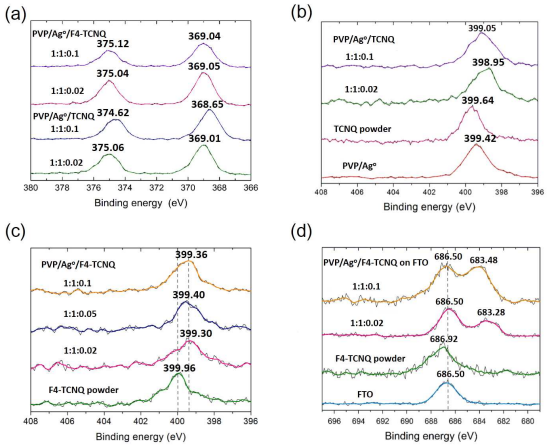

Figure 4. XPS binding energy spectra for (a) silver, (b) nitrogen in PVP/AgNPs/TCNQ, (c) nitrogen and (d) fluorine and in PVP/AgNPs/F4-TCNQ composites with varying weight ratios.

RSC Advances Accepted Manuscript

This journal is © The Royal Society of Chemistry 2012

On the other hand, the binding energy of nitrogen in the PVP/Ag^{o}/TCQs composite system was found to decrease, except for PVP/Ag^{o}/TCNQ=1:1:0.1 (wt. ratio), as shown in Fig.4 (b) and (c). In particular, two different fluorine binding energies were clearly observed in PVP/Ag^{o}/F4-TCNQ coated on FTO. These peaks may be ascribed to F4-TCNQ^{2-} and FTO, respectively. These changes in binding energies could indicate partial electron transfer from silver to TCQs molecules. Therefore, it is expected that the surface of the silver nanoparticles should have a partial positive charge, and hence should actively interact with the olefin molecules.

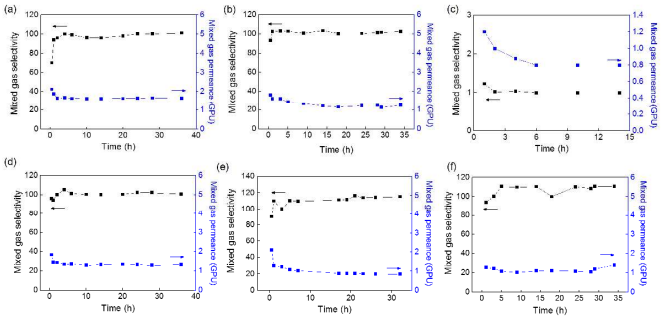

Figure 5. Separation performances of the different PVP/AgNPs/TCQs membranes with various compositions for 50:50 (v/v) propylene/propane mixture. (a) PVP/AgNPs/TCNQ=1:1:0.02, (b) PVP/AgNPs/TCNQ=1:1:0.05,(c) PVP/AgNPs/TCNQ = 1:1:0.1, (d) PVP/AgNPs/F4-TCNQ = 1:1:0.02, (e) PVP/AgNPs/F4-TCNQ = 1:1:0.05 and PVP/AgNPs/F4-TCNQ = 1:1:0.1

Olefin separation performance

The propylene/propane separation performances of the PVP/Ag^{o}/TCQs nanocomposite were evaluated as shown in Fig. 5. The mixed selectivity of propylene over propane, which is defined as the propylene concentration ratio of the permeate to the feed, was no separation performance for the neat PVP membrane with a permeance of about 0.01 GPU.

Interestingly, most of the PVP/AgNPs/TCQs composite membranes showed a dramatic increase in the selectivity above 100, and increase in the gas permeance by nearly 10,000% up to 1.8 GPU. The maximum selectivity of up to 112 was obtained in PVP/AgNPs/F4-TCNQ=1:1:0.05 (wt. ratio), as shown in Fig. 6 (e). The observed increase in selectivity and gas permeance clearly indicates facilitated olefin transport due to the interactions of propylene with the positively induced charge density on the surface of AgNPs. Furthermore, the stability of the carrier AgNPs was also tested, which indicate stable separation performance for 36 h of continuous operation, as shown in Fig. 4. As was confirmed previously by theoretical *ab initio* calculations,[8a] the carrier activity is a consequence of reversible interactions of propylene with partially positively charged surface of the Ag nanoparticles induced by TCQs molecules. However, separation performance was not achieved in PVP/AgNPs/TCNQ=1:1:0.1 (wt. ratio), upon using nanorod-shaped AgTCNQ as an olefin carrier (Fig.6 (c)). This suggests that the reversible interaction with olefin is not observed in case of $Ag^{+}TCNQ^{-}$, rather it occurs when partially positively charged AgNPs, *i.e.*, $AgNPs^{\delta+}$ $TCQ^{\delta-}$ is used as the olefin carrier.

Conclusions

In summary, the PVP/AgNPs/TCQs composite membranes showed markedly improved separation performance with the maximum mixed gas selectivity of 110 for propylene/propane (50/50 v/v) mixture, indicating that these are unprecedented highly olefin permselective membranes that use silver metal as an olefin carrier. The observed improvement in the separation performance can be mostly associated with the synergistic effect of (1) the high positive charge density of the surface of the silver nanoparticles induced by the addition of TCQs, and (2) the high carrier concentration with large surface area that facilitates interactions with olefin molecules. Therefore, it can be concluded that the high charge density of the silver nanoparticles plays the most important role in enhancing the separation performance of olefin/paraffin mixtures.

Acknowledgements

This work was supported by an Energy Efficiency & Resources of the Korea Institute of Energy Technology Evaluation and Planning (KETEP) grant funded by the Korean government Ministry of Trade, Industry and Energy (20122010100040). This work was also supported by Korea CCS R&D Center through the National Research Foundation of Korea (NRF) funded by the Ministry of Science, ICT and Future Planning. Y. S. Kang also acknowledges the Basic Science Research Program through the National Research Foundation of Korea (NRF) grant funded by the Ministry of Science, ICT and Future Planning of Korea for the Center for Next Generation Dye-sensitized Solar Cells (No. 2011-0001055). This research was also supported by a 2013 Research Grant from Sangmyung University.

Notes and references

[a] Department of Energy Engineering, Hanyang University, Seoul 133-791 (Republic of Korea), E-mail: kangys@hanyang.ac.kr

[b] Department of Chemistry, Sangmyung University, Seoul 110-743 (Republic of Korea), E-mail: swkang@smu.ac.kr

1 a) N. Du, H. B. Park, M. M. Dal-Cin, M. D. Guiver, *Energy Environ. Sci.*, 2012, **5**, 7306; b) M. D. Guiver and Y. M. Lee, *Science*, 2013, **339**, 284; c) A. M. W. Hillock, S. J. Miller, W. J. Koros, *J. Membr. Sci.*, 2008, **314**, 193; d) D. Vuono, J. Henkel, J. Benecke, T. Y. Cath, T. Reid, L. Johnson, J. E. Drewes, *J. Membr. Sci.*, 2013, **446**, 34.

2 a) P. Bernardo, E. Drioli, G. Golemme, *Ind. Eng. Chem. Res.*, 2009, **48**, 4638; b) W. J. Koros, *J. Membr. Sci.*, 2007, **300**, 1.

3 a) T. C. Merkel1, B. D. Freeman, R. J. Spontak, Z. He, I. Pinnau, P. Meakin, A. J. Hill, *Science*, 2002, **296**, 519; b) Y. C. Hudiono, T. K. Carlisle, A. L. LaFrate, D. L. Gina, R. D. Noble, *J. Membr. Sci.,* 2011, **370**, 141; c) K. Simons, K. Nijmeijer, M. Wesslingm, *J. Membr. Sci.*, 2009, **340**, 214.

4 a) K. M. Sundaram, M. M. Shreehan, E. F. Olszewski,*Kirk-Othmer Encyclopedia of Chemical Technology*, Wiley, New York, ed. 4, 1995;b) R. L. Grantom, D. J. Royer, *Ullmann's Encyclopedia of Industrial Chemistry*, VCH, New York, ed. 5, 1987;c) K. Wang, E. I. Stiefel, *Science*, 2001, **291**, 106.

5 a) C. Staudt-Bickel, W. J. Koros, *J. Membr. Sci.*, 2000, **170**, 205; b) I. G. Giannakopoulos, V. Nikolakis, *Ind. Eng. Chem. Res.*, 2004, **44**,

RSC Advances Accepted Manuscript

226; c) M. L. Chng, Y. Xiao, T- S. Chung, M. Toriida, S. Tamai, *Carbon*, 2009, **47**, 1857.

6 Y. S. Kang, J. H. Kim, J. Won, H. S. Kim in Material Science of Membranes for Gas and Vapor Separations (Eds.: Y. Yampolski, I. Pinnau, B. D. Freeman), Wiley, Chichester, 2006, Chapter 16.

7 a) H. Ishii, K. Sugiyama, E. Ito, K. Seki, *Adv. Mater.*,1999, **11**, 605; b) G. Heimel, L. Romaner, E. Zojer, J. Bredas, *Acc. Chem. Res.*, 2008, **41**, 721.

8 a) Y. S. Kang, S.W. Kang, H. Kim, J. H. Kim, J.Won, C. K. Kim, K.Char, *Adv. Mater.*, 2007, **19**, 475; b) I. S. Chae, S. W. Kang, J. Y. Park, Y-G. Lee, J. H. Lee, J. Won, Y. S. Kang, *Angew. Chem. Int. Ed.*, 2011, **50**, 2982.

9 S. W. Kang, J. H. Kim, J. Won, Y. S. Kang, *J. Membr. Sci.*, 2013, **445**, 156.

10 a) G. Zotti, B. Vercelli, *Anal. Chem.,* 2008, **80**, 815; b) S. Panja, U. Kadhane, J. U. Andersen, A. I. S. Holm,P. Hvelplund, M-B. S. Kirketerp, S. B. Nielsen, K. Støchkel, *J. Chem. Phys.*, 2007, **127**, 124301;c) L. R. Melby, R. J. Harder, W. R. Hertler, W. Mahler, R. E. Benson, W. E. Mochel, *J. Am. Chem. Soc.*, 1962, **84**, 3374; d) V. Bellec, M. G. De Backer, E. Levillain, F. C. Sauvage, B. Sombret, C. Wartelle, *Electrochem. Commun.*, 2001, **3**, 483.

11 a) L. Ren, L. Fu, Y. Liu, S. Chen, Z. Liu, *Adv. Mater.*, 2009, **21**, 4742; b) J. Xiao, Z. Yin, Y. Wu, J. Guo, Y. Cheng, H. Li, Y. Huang, Q. Zhang, J. Ma, F. Boey, H. Zhang, Q. Zhang, *Small*, 2011, **7**, 1242; c) K. Xiao, J. Tao, A. A. Puretzky, I. N. Ivanov, S. T. Retterer, S. J. Pennycook, D. B. Geohegan, *Adv. Funct. Mater.*, 2008, **18**, 3043.

RSC Advances Accepted Manuscript

 This journal is © The Royal Society of Chemistry 2012